Food Hydrocolloids 160 (2025) 110741

Contents lists available at ScienceDirect

Food Hydrocolloids

journal homepage: www.elsevier.com/locate/foodhyd

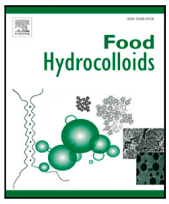

Casein network formation at oil–water interfaces is reduced by β-casein and increased by Ca^{2+}

A. de Groot [a,b], E. Bijl [b], L.M.C. Sagis [a,*]

[a] Laboratory of Physics and Physical chemistry of foods, Wageningen University, Bornse Weilanden 9, Wageningen, 6708 WG, The Netherlands
[b] Dairy Science and Technology, Food Quality and Design group, Wageningen University, Bornse Weilanden 9, Wageningen, 6708 WG, The Netherlands

ARTICLE INFO

Keywords:
Casein
Interfacial network
General stress decomposition
Calcium sensitivity
Lissajous plots

ABSTRACT

Mixtures of bovine caseins can serve as a benchmark for understanding the functionality of microbial-based recombinant caseins at oil–water interfaces. In this work we show that, in the presence of Ca^{2+}, the individual casein fractions form viscoelastic networks at the oil–water interface with comparable stiffness. In the absence of Ca^{2+}, α_{s2}- and β-casein interfacial network formation was strongly inhibited over the full deformation regime. For α_{s1}-casein, the network stiffness was increased in the absence of Ca^{2+} at small deformations (<15%), but at large deformations (>50%) it was completely disrupted, to a similar stiffness as α_{s2}- and β-casein. The interfacial structure formed by κ-casein was largely unaffected by Ca^{2+} due to limited phosphorylation. We hypothesize that the differences between calcium-sensitive caseins lie in the conformation they assume at the interface. Both α_{s2}- and β-casein adsorb in a train-tail conformation with a tail extending into the aqueous bulk phase, whereas α_{s1}-casein adsorbs in a loop-train conformation, with a loop that extends less into the bulk phase. The tail-train configuration is hypothesized to increase the inter-molecular Ca^{2+} bridging thereby increasing the interfacial stiffness of α_{s2}- and β-casein.

Blending the casein fractions revealed a strong negative effect of β-casein on the interfacial modulus, which was more pronounced at a higher concentration. The presence of Ca^{2+} remained important for interfacial network formation of a casein blend. Without Ca^{2+}, the interfacial network was less stiff, more viscous, and behaved like a 2d polymer solution.

With this work we showed that casein interfacial network formation at oil–water interfaces is mediated by Ca^{2+} bridging. Blending the different casein fractions decreased the interfacial viscoelastic properties through the presence of β-casein. These results indicate that future work on recombinant caseins should focus on single genetic variants, since a blend of variants will likely decrease interfacial functionality.

1. Introduction

Caseins play a key role in the environmental impact of our diet, therefore it is important to understand their functionality in food. Dairy has a big impact on the environment (Food and Agriculture Organization, 2010; Poore & Nemecek, 2018), hence industry and academia investigate plant-based proteins and microbial-based recombinant proteins as casein alternatives. The latter are produced using microbial cells as production hosts of caseins by inserting a casein gene using recombinant DNA technology in a process known as precision fermentation. Replacing casein with plant proteins is not trivial because many plant proteins lack nutritional value and functionality (Diaz-Bustamante et al., 2023). Precision fermented proteins provide a better alternative, since they contain nutritionally similar components and potentially improve functionality, although limited studies are available (Diaz-Bustamante et al., 2023). To correctly assess the functionality of precision fermented protein we need a benchmark and an understanding of how casein functionality within dairy products is established.

The milk protein fraction in bovine milk consists of 80% caseins. The individual casein fractions (α_{s1}-, α_{s2}-, β-, & κ-casein) in this milk are assembled into supramolecular structures called casein micelles. Casein micelles are held together by interactions between the individual fractions and by interactions with inorganic calcium phosphate. Each molecule forms hydrogen bonds or hydrophobic interactions with other casein molecules while they can also bind calcium phosphate nanoclusters. The inorganic calcium phosphate interacts with the phosphoserine residues of α_{s1}-, α_{s2}-, and β-casein thereby forming a

* Corresponding author.
E-mail address: leonard.sagis@wur.nl (L.M.C. Sagis).

https://doi.org/10.1016/j.foodhyd.2024.110741
Received 18 June 2024; Received in revised form 1 October 2024; Accepted 11 October 2024
Available online 21 October 2024

protein cluster (Horne, 2020). The presence of micelles poses one of the biggest challenges finding alternative protein sources to produce dairy. Many dairy products rely heavily on casein micelles for their structure (e.g. cheese) while the alternative proteins have difficulty forming similar structures. With plant-based proteins, which are mostly globular proteins, it is impossible to form similar micellar structures, and precision fermented casein will likely lack the phosphorylation required for micelle formation (Hansson et al., 1993; Hettinga & Bijl, 2022; Loch et al., 2016). However, not all products necessarily require micellar casein for their formation and/or stabilization.

Emulsions belong to the latter category and are therefore a great opportunity for applying alternative proteins to casein. Since casein is an important protein in stabilizing dairy emulsions, the alternative should be selected carefully. After homogenization of the emulsion, casein is the most abundant protein at the oil–water interface of a milk-fat globule (Cano-Ruiz & Richter, 1997; Darling & Butcher, 1978; Iametti et al., 1997; Mccrae, 1994). At the interface it forms a viscoelastic network (Dickinson et al., 1988; Fainerman et al., 2020; Husband et al., 1997; Wüstneck et al., 2012; Zhou et al., 2022) that is essential for emulsion stability (Jin et al., 2021; Langevin, 2000; Miller et al., 2010; Sagis, 2011). Even though 95% of the casein is assembled into micelles (Dumpler, 2018; Fox et al., 2015), the smaller constituents (the other 5%) are dominant in forming a viscoelastic network at the oil–water interface (Zhou et al., 2022). In particular for precision fermented casein, we need to further study the underlying principles that govern oil–water stabilization by small casein constituents as was also done for air–water interfaces (de Groot et al., 2024). Precision fermentation will produce highly similar caseins to the bovine casein genetic variants but it is not yet known what genetic variant is most suitable for application in emulsions and whether phosphorylation is necessary for interface stabilization.

This study uses bovine caseins to study the interfacial functionality of individual casein fractions to create a benchmark for alternative proteins. Furthermore, the effect of mixing fractions will be studied to map the interactions between casein fractions. Since, Ca^{2+} plays such a vital role in the casein chemistry, simulated milk ultrafiltrate buffer with and without Ca^{2}+ was used to probe Ca^{2+} mediated interactions within the interface. The interfacial functionality was studied with drop tensiometry by first studying the adsorption behavior followed by oscillating drop tensiometry. Oscillations where performed within the small- and large amplitude regime and analyzed with the general stress decomposition (de Groot et al., 2023). This study can serve as a road map for the application of precision fermented caseins in emulsions.

2. Materials & methods

2.1. Materials

Individual α_{s1}-, α_{s2}-, β-, & κ-casein fractions were prepared in collaboration with Those Vegan Cowboys (Gent, Belgium), identical to the study of de Groot et al. (2024). The fractions were obtained by column separation and dialyzed against MilliQ water (Veolia, Ireland). Medium chain triglyceride oil was obtained from IMCD (Netherlands) and all other chemicals (Sigma-Aldrich, USA) were used as received.

2.2. Protein content

The nitrogen content was measured in a flash EA 112 NC Analyzer (Thermo Fischer Scientific INC, USA). With a nitrogen-to-protein conversion factor of 6.38 the protein content was calculated.

2.3. Sample composition

The composition of each casein fraction was calculated from the peak area of reverse-phase high-performance liquid chromatography separation (RP-HPLC, Thermo Science Ultimate 3000; Waltham, USA) with the method developed by Bonfatti et al. (2008), de Vries et al. (2015). The protocol was identical to what was done by de Groot et al. (2024). The chromatograms (SI, Fig. S1) were analyzed in Chromeleon 7.1.2 where the ratio between the individual peak areas and total peak area was used as the relative abundance (see Table 1).

2.4. Sample preparation

2.4.1. Buffer preparation

Simulated milk ultrafiltrate (SMUF) was prepared based on the composition proposed by Jennes and Koops (1962). In short, SMUF was prepared by mixing 50x concentrated stock solutions (see Table 2) in equal amounts with MilliQ water. After dissolving for 30 min, the pH was adjusted to 6.7 with KOH and stored for a maximum of 7 days in the fridge. Modified SMUF buffer was used to evaluate the effect of Ca^{2+} in SMUF by replacing $CaCl_2 \cdot H_2O$ by an equimolar amount of 2.1% (w/v) NaCl.

2.4.2. Preparation of protein solution

Casein fractions were stored in the freezer at −21 °C, before the casein solution was thawed to room temperature, whereafter it was diluted in buffer to obtain the desired protein concentration (w/v). A blend of several casein fractions was prepared by pipetting individual droplets of casein fraction into a tube -without mixing them- and subsequently adding the correct amount of buffer to create a homogeneous mixture. Blends of casein fractions were mixed in the ratio as they occur in milk 4:1.1:3.8:1.3 (Davies & Law, 1977).

2.5. Interfacial properties

The interfacial properties were characterized by creating a 30 mm2 pendant drop of protein solution in medium-chain triglyceride (MCT) oil at the tip of a G18 needle. The droplet shape was recorded and fitted to the Young–Laplace equation with an automated drop tensiometer (ADT, Teclis Scientific, France) to calculate the surface tension.

2.6. Interface equilibration

Surface tension development of the protein solution was followed for 3 h and the adsorption phase was fitted with a first-order relaxation equation, as proposed by Graham and Phillips (1979), described by

$$\gamma_{ads}(t) = \gamma_{\infty} + (\gamma_{t0} - \gamma_{\infty}) a e^{-\frac{(t-t_0)}{t_{ad}}} \quad (1)$$

Here, t is time and t_0 is the estimated transition time between adsorption and rearrangement with a relative contribution a for adsorption. The surface tension at t_0 is γ_{t0} and the estimated asymptotic surface tension is γ_{∞}. Estimation of γ_{∞} was done by averaging the last 10 surface tension measurements of equilibration. Estimation of t_0 and thereby γ_{t0} was done by plotting the $\ln(\gamma(t))$ vs t and calculating the maximum curvature. The point of maximum curvature was assumed to be the transition regime from adsorption to rearrangement. The rearrangement regime was then fitted with power law behavior, as also can be done for bulk aging processes (White, 2006):

$$\gamma_{re}(t) = bt^{-r} \quad (2)$$

Here, $\gamma_{re}(t)$ is the surface tension in the rearrangement regime, b is a scaling factor and r the dimensionless rate of rearrangement exponent.

Table 1
Casein fraction composition based on RP-HPLC.

	α_{s1}-casein (%)	α_{s2}-casein (%)	β-casein (%)	κ-casein (%)	Unknown (%)
α_{s1}-casein fraction	92.5	6.7	–	–	0.8
α_{s2}-casein fraction	8.3	90.8	–	–	0.9
β-casein fraction	–	–	98.5	–	1.5
κ-casein fraction	5.1	1.8	11.6	74.2	7.4

Table 2
Composition of SMUF stock solutions, based on (Jennes & Koops, 1962).

	Mineral	Concentration (%, w/v)
Stock 1	KH_2PO_4	7.90
	$K_3C_6H_8O_7 \cdot H_2O$	5.45
	$Na_2C_6H_8O_7 \cdot 2H_2O$	8.95
	K_2SO_4	0.90
Stock 2	K_2CO_3	1.5
	KCl	3.39
Stock 3	$MgCl_2$	1.53
	$CaCl_2 \cdot H_2O$	6.60

2.7. Interfacial dilatational rheology

After 3 h equilibration, the droplet was subjected to oscillatory deformations in the form of frequency or strain sweeps. Frequency sweeps where applied at 0.00333–0.1 Hz and a strain of 0.125. Strain sweeps where applied at 0.02 Hz and 0.03–0.6 strain. Between a set of oscillations, at least one period of waiting time was applied. Each set of oscillation consisted of five oscillatory cycles applied by a motor drive syringe, and for analysis only the middle 3 cycles where used.

2.7.1. Analysis of interfacial dilatational rheology

Frequency sweeps were analyzed by fitting the storage modulus (E'_d) to a power law ($E'_d \sim \omega^n$), where ω is the frequency and n is the exponent. Additionally, the complex modulus was fitted to the Lucassen-van den Tempel (LVDT) model, where $E^* = \sqrt{E'^2_d + E''^2_d}$ is given by

$$E^* = \epsilon_0 \frac{1 + \zeta + i\zeta}{1 + 2\zeta + 2\zeta^2}, \quad \zeta = \sqrt{\frac{\upsilon_D}{2\omega}} \tag{3}$$

Here the Gibbs elasticity is denoted by ϵ_0 and the characteristic frequency of diffusive transport of protein between bulk and interface is given by υ_D. Similar to the LVDT model, the Maxwell model was fitted to the complex modulus by

$$E^* = \frac{E\eta^2\omega^2 + i\omega E^2\eta}{\eta^2\omega^2 + E^2} \tag{4}$$

Here, E is the elastic modulus of a purely elastic spring and η is the viscosity of a purely viscous damper.

The stress response of strain sweeps was analyzed with the general stress decomposition (GSD) (de Groot et al., 2023). GSD analyses intracycle nonlinearities by decomposition into odd harmonics and even harmonics of a Fourier series. The odd and even harmonics were visualized by plotting intracycle strain ($(A(t) - A_0)/A_0$) versus surface pressure ($\Pi = \gamma(t) - \gamma_0$). Here, the odd harmonics show network interactions and the even harmonics show nonlinearities as a result of changes in surface density (de Groot et al., 2023). The network properties can be described by the initial stiffness of the network ($E_{\tau_{1M}}$), the overall stiffness ($E_{\tau_{1L}}$), the stiffening factor S based on $E_{\tau_{1M}}$ and $E_{\tau_{1L}}$, and the total dissipated energy ($U_{d\tau 2}$). Like in bulk rheology viscoelastic plasticity can be defined with the dissipation ratio (Φ) as defined by Ewoldt et al. (2010). Nonlinearities in the intracycle surface density changes are quantified by a secant modulus (E_{τ_4}), a shift (γ_s), and the dissipated energy ($U_{d\tau 3}$) as calculated by:

$$E_{\tau_{1M}} = \frac{\sum_{k=0}^{i/2}(2k+1)b'_{2k+1}}{\epsilon_0} \tag{5}$$

$$E_{\tau_{1L}} = \frac{\sigma_{max}}{\epsilon_0}, \quad \sigma_{max} = \sum_{k=0}^{i/2} b'_{2k+1}(-1)^k \tag{6}$$

$$S = \frac{E_{\tau_{1L}} - E_{\tau_{1M}}}{E_{\tau_{1L}}} \tag{7}$$

$$U_{d\tau 2} = \pi\epsilon_0^2 E_1^{\varepsilon} \tag{8}$$

$$E_{\tau_4} = \frac{\sum_{k=0}^{i/2} 2d'_{4k+2}}{\epsilon_0} \tag{9}$$

$$\gamma_s = d'_0 \tag{10}$$

$$U_{d\tau 3} = 2\epsilon_0^2 \sum_{k=1}^{i/2} \frac{E_{2k\tau 3} * k}{k^2 - 1/4} \tag{11}$$

$$\Phi = \frac{\pi\epsilon_0^2 E_1^{\varepsilon}}{4\sigma_{max}} \tag{12}$$

Here b'_{2k+1}, a'_{2k+1}, c'_{2k}, and d'_{2k} are the Fourier coefficients of the stresses τ_1, τ_2, τ_3, and τ_4. The analysis was performed with a MATLAB (2022b) script that includes only harmonics (I_n) with an intensity >3% relative to the first harmonic, i.e. $I_n/I_1 > 0.03$.

2.8. Calculation of hydrophobicity along amino acid chain

The hydrophobicity along the amino acid chain of α_{s1}-, α_{s2}-, β-, and κ-casein was calculated according to Dalgleish (1993). The hydrophobicity of each amino acid according to Cowan and Whittaker (1990) was used to calculate an average segment hydrophobicity by summing the contributions over 7 amino acids (N+3) to (N−3). Iteration over all amino acid residues maps an averaged hydrophobicity over each amino acid chain of each casein fraction.

2.9. Statistical analysis

A students T-test with unequal variance was used to identify significant differences. A p-value < 0.05 was considered significant.

3. Results & discussion

3.1. Adsorption behavior of casein fractions and the effect of Ca^{2+}

The interfacial functionality of casein is highly dependent on the type of casein (CN) and presence of Ca^{2+}, as was shown for air–water interfaces (de Groot et al., 2024). Therefore, we first characterized each casein fraction at the oil–water interface in the presence and absence of Ca^{2+}, starting with the adsorption kinetics. Amphiphilic proteins can adsorb at and orient themselves on the interface to reduce surface tension. After the initial adsorption phase, in which a relatively fast drop in surface tension can be observed, a second stage is often reached where the surface tension is slowly decreasing due to structural rearrangements within the interface.

The adsorption stage in Fig. 1 A is quantified with a first order relaxation equation Eq. (1) (Graham & Phillips, 1979) with the adsorption time (t_{ad}) as a characteristic time for adsorption. The adsorption time

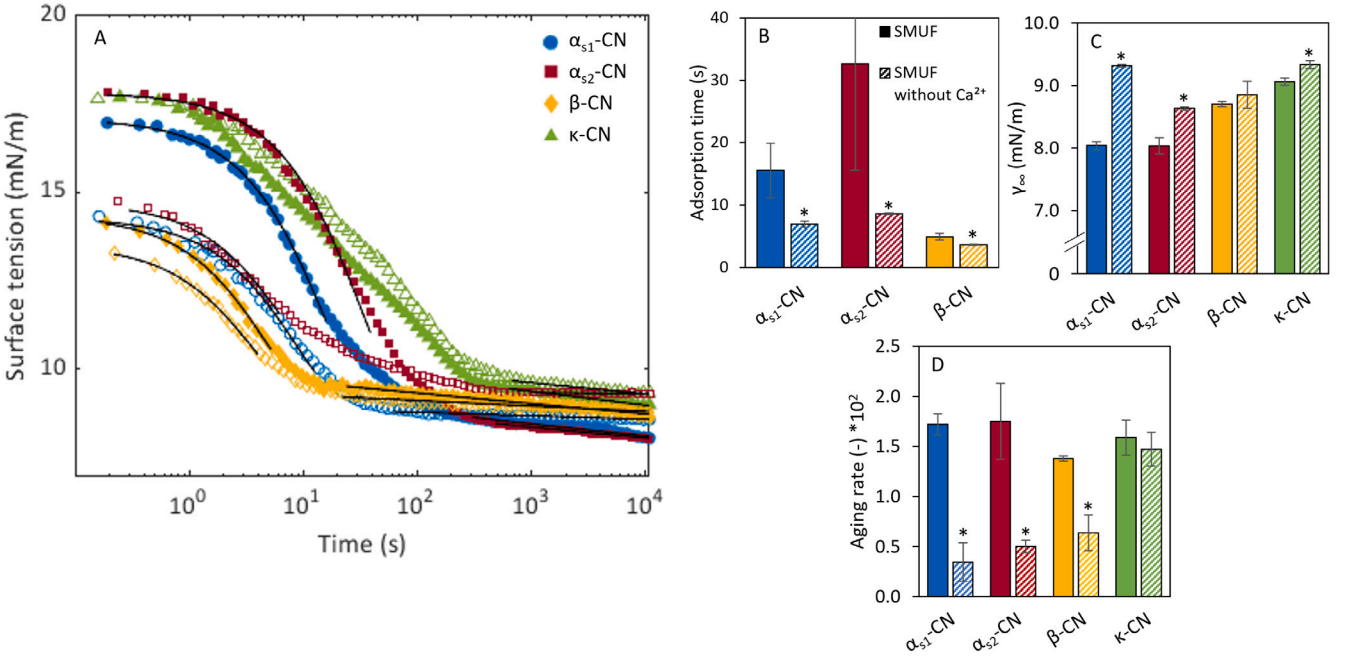

Fig. 1. Representative equilibration curves (A) and corresponding adsorption time (t_{ad}) (B), asymptotic surface tension (C), and dimensionless aging rate exponent (D) of casein fractions at oil–water interfaces. The adsorption regime of the casein fractions is fitted with Eq. (1) (black line) and the aging process is fitted with Eq. (2) (black line) in SMUF (filled symbols) and SMUF without Ca^{2+} (open symbols). Significant differences between samples with and without Ca^{2+} are indicated with an asterisk.

is plotted in Fig. 1 B where we see that the adsorption time for α_{s1}-CN, α_{s2}-CN, and β-CN significantly increases with the addition of Ca^{2+}. Probably, the caseins self-associate under the influence of Ca^{2+} (Aoki et al., 1985; Harton & Shimizu, 2019; Horne & Dalgleish, 1980; Li et al., 2019, 2020) which slows down adsorption to the interface. For κ-CN, the equilibration curve was nearly independent on the presence of Ca^{2+}. This was expected since κ-CN is known for its insensitivity to Ca^{2+} (Swaisgood, 1993; Thorn et al., 2015), the major isoform has only one phosphoserine residue (Bijl et al., 2019). The κ-CN adsorption could not be described by first order relaxation Eq. (1). Probably, the κ-casein adsorption is governed by multiple processes with each their own adsorption time. We expect that this is related to different isoforms of κ-CN, the isoforms vary slightly in molecular structure (Holland et al., 2006) and therefore in adsorption time.

The rearrangement regime was quantified by comparing the asymptotic surface tension and by fitting the rearrangement regime with power-law behavior Eq. (2) as is also done for bulk aging processes (White, 2006). The samples with Ca^{2+} show a lower γ_∞ in Fig. 1 D, which could be indicative of a higher surface density. Probably, the Ca^{2+} mediated attraction between casein molecules results in a more efficient stacking of the casein molecules within the interface. The aging exponent r is plotted in Fig. 1 C, and is significantly higher for the samples with Ca^{2+}. This indicates that the interface is still showing significant aging for the samples with Ca^{2+}, even after 3 h. Whereas the samples without Ca^{2+}, appear to reach (quasi) equilibrium after at a much earlier stage, indicating that by adding Ca^{2+} the molecular mobility is significantly decreased, most likely by increased surface density and in-plane connectivity.

3.2. *Viscoelastic properties of Casein fractions and the effect of* Ca^{2+}

The viscoelastic properties of the interfacial structure were characterized by dilatational amplitude sweeps. In Fig. 2 A and B, the initial modulus $E_{\tau 1M}$ is shown in SMUF with and without Ca^{2+}. In SMUF with Ca^{2+}, the interfacial modulus of all casein fractions is similar (plot A). Here, α_{s1} forms the stiffest interface followed by α_{s2}- and κ-CN. Interestingly, β-CN has the lowest modulus which is contrary to what was seen at air–water interfaces where it had the highest modulus (de Groot et al., 2024). This emphasizes the fundamental differences between air–water and oil–water interfaces and the need for separate characterization. Oil has a lower hydrophobicity than air and thereby induces less strong capillary forces, additionally the hydrophobic protein fragments are thought to protrude further into an oil-based hydrophobic phase (Bergfreund et al., 2021a), and finally oil has a higher dielectric constant which affects the range and strength of electrostatic and van der Waals interactions within the interfacial structure. The effect of hydrophobicity has been shown to significantly affect the surface tension and modulus of proteins (Bergfreund et al., 2021a, 2021b).

When we compare the interfacial modulus in the absence of Ca^{2+} we see drastic changes for α_{s1}-CN, α_{s2}-CN, and β-CN. κ-CN is less affected by the presence of Ca^{2+} as previously explained for the adsorption phase. Both α_{s2}-CN and β-CN have a lower initial modulus in the absence of Ca^{2+}. This shows that Ca^{2+} is an important component of the interfacial network formed by α_{s2}-CN or β-CN. The α_{s2}-CN interface even exhibits nearly plastic behavior as witnessed by the high dissipation ratio $\sim$ 0.75 in plot D. This value is close to that of a Newtonian fluid where $\Phi = \frac{\pi}{4} \approx 0.785$ (Ewoldt et al., 2010) and there is apparently hardly any network formation for α_{s2}-CN in the absence of Ca^{2+}. For β-casein, the initial modulus is low but the dissipation ratio also remains low at $\sim$ 0.15 showing that the network is very weak but highly flexible as there is no change in dissipation ratio even at 0.6 strain. This confirms the study of Chrysanthou et al. (2023) who showed that β-casein in phosphate buffer (without Ca^{2+}) forms a weak gel with limited in-plane diffusion.

For α_{s1}-CN, the initial interfacial stiffness ($E_{\tau 1M}$) at low deformations is high in the absence of Ca^{2+} ($\sim$ 6 vs $\sim$ 8 mN/m). However, from strain 0.15 to 0.6 the modulus decreases progressively and reaches even lower values than with Ca^{2+} ($\sim$ 4 vs $\sim$ 2 mN/m at 0.6) and comparable to α_{s2}-CN and β-CN. This shows that Ca^{2+} is important for retaining interfacial stiffness in the large deformation regime for all three calcium sensitive caseins. The decreasing modulus of α_{s1}-CN is accompanied

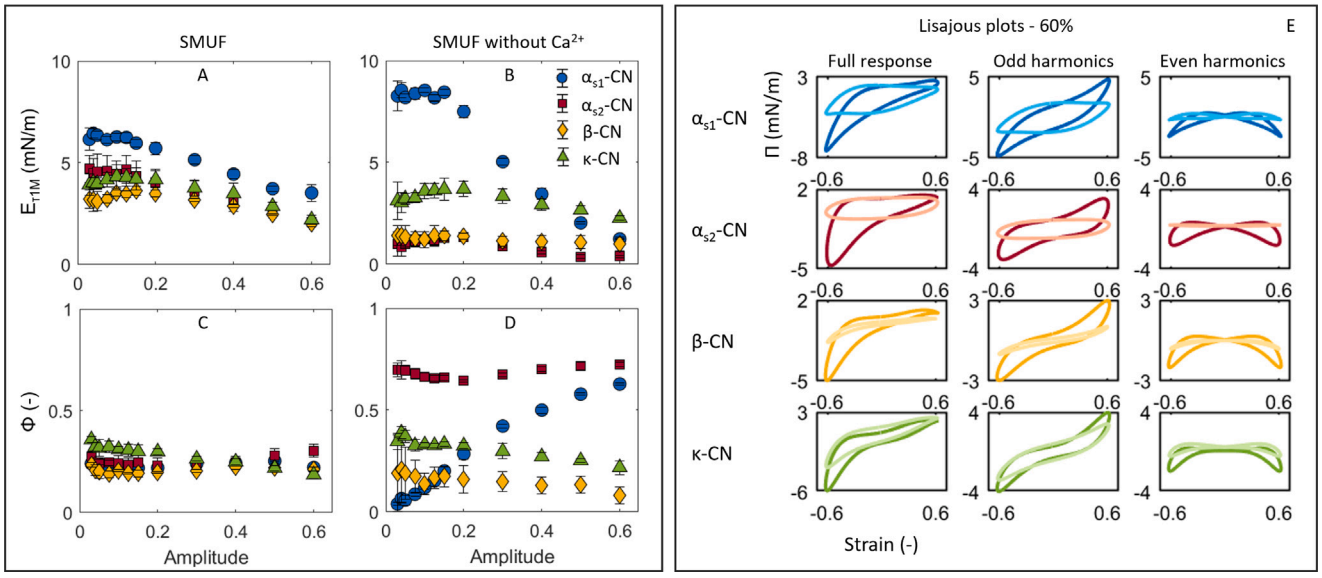

Fig. 2. A strain sweep of α_{s1}- (blue circle), α_{s2}- (red square), β- (yellow diamond), & κ-casein (green triangle) at 0.02 Hz. Quantification in the left panel is performed with the general stress decomposition where the initial modulus ($E_{\tau 1L}$) and (Φ) are plotted versus the amplitude in SMUF (A & C) and in SMUF without Ca^{2+} (B & D). The right panel (E) shows the decomposed Lissajous plots of each casein fraction in SMUF (dark) and in SMUF without Ca^{2+} (light) at 60% deformation.

Table 3
The dilatational storage modulus at 5% deformation for binary blends of the four casein fractions at 0.01% in the ratio as they occur in milk 4:1.1:3.8:1.3 (Davies & Law, 1977). In each row the modulus of the 'pure' fraction is shown in white and the corresponding blends are colored red for a reduction in modulus and colored green for an increase. Significant differences are labeled with an asterisk.

E'_d at 0.01%	α_{s1}-CN	α_{s2}-CN	β-CN	κ-CN
α_{s1}-CN	6.4	6.9	4.9	6.7
α_{s2}-CN	6.9*	4.7	2.5*	5.5
β-CN	4.9	2.5	3.3	2.5
κ-CN	6.7*	5.5	2.5	4.4

Table 4
The storage modulus at 5% deformation for β-CN binary blends with the other three casein fractions at 0.1% in the ratio as they occur in milk 4:1.1:3.8:1.3 (Davies & Law, 1977). The modulus of β-CN is shown in white and the corresponding blends are colored red for a reduction in modulus and colored green for an increase. Significant differences are labeled with an asterisk.

E'_d at 0.1%	α_{s1}-CN	α_{s2}-CN	β-CN	κ-CN
β-CN	2.8	2.4	3.1	2.8

by and increasing dissipation ratio from 0.05 to 0.6. This shows that the interfacial network is broken down and the viscoelastic response is increasingly plastic. We conclude that the absence of Ca^{2+} causes the casein interfacial network to be less stiff at large deformations.

In the Lissajous curves at 0.6 strain (Fig. 2 E), we also observe a highly viscous response for the network interactions (i.e. odd harmonics) of both α_{s1}- and α_{s2}-CN in the absence of Ca^{2+}. The β-CN stabilized interface shows a predominately elastic Lissajous curve with a low slope when Ca^{2+} is absent. For these three caseins at 0.6 strain, the contribution from the even harmonics is also close to zero. At these high strains a lot of new interface is created in expansion, and bulk-interface exchange will be significant, thereby in large part negating the intracycle surface density changes. To explain the differences between α_{s1}-CN and α_{s2}- & β-CN we need to study the protein configuration at the interface.

Since casein fractions are considered unstructured, the hydrophobicity over the amino acid sequence gives a good indication of the conformation at an interface (Dalgleish, 1993), except for κ-CN. In Fig. 3, the hydrophobicity of each casein fraction is calculated from their amino acid sequence. This figure shows several distinctly more hydrophilic regions in the casein fractions which confirms what was previously shown in literature (Dalgleish, 1993; Dickinson et al., 1997; Huppertz, 2013). κ-CN conformation is very well studied with respect to casein micelles, literature shows that κ-CN has a distinctly hydrophilic C-terminal region (Bijl et al., 2019; de Kruif & Zhulina, 1996; Walstra & Jennes, 1984). Remarkable is the high phosphorylation in the hydrophilic regions of α_{s1}-CN, α_{s2}-CN, and β-CN, which are known to dominate calcium-induced network formation (Aoki et al., 1992). Interestingly, α_{s2}-CN, and β-CN each have a more hydrophilic block at one end of their sequence, and are therefore likely to assume a train-tail configuration, with the hydrophilic tail protruding into the aqueous phase. In contrast, α_{s1}-CN has a large hydrophilic block more towards the middle of the sequence, which makes it likely that this protein adsorbs in a train-loop-train configuration. The dangling tail that α_{s2}-CN, and β-CN each have protruding into the hydrophilic solution would explain the higher interfacial thickness of α_{s2}-CN, and β-CN compared to α_{s1}-CN observed by Dalgleish (1993), as was already suggested for β-CN by Dickinson et al. (1997). This tail contains the phosphoserine residues and therefore facilitates the formation of Ca^{2+} bridges between molecules as suggested for β-CN by Velev et al. (1998). On the other hand, α_{s1}-CN has a train-loop-train configuration that is not able to reach as far into solution (Dalgleish, 1993; Dickinson et al., 1997) and Ca^{2+} bridging is more likely to occur within the same molecule as shown in Fig. 3 B. Hence, we hypothesize that the train-loop-train configuration in α_{s1}-CN reduces its capacity to form Ca^{2+} induced interfacial networks. Therefore, the presence of Ca^{2+} does not increase the modulus of α_{s1}-CN, as it does for the other two proteins. Why the addition of Ca^{2+} actually reduces the modulus at low strain amplitude, and renders the structure less sensitive to disruption at high strain, is not yet clear. Without Ca^{2+}, the elasticity we observe is the result of a weak network formed by in-plane interactions between the train sections of the protein configuration. The adsorption measurements show that in the presence of calcium α_{s1}-CN adsorbs considerably slower to the oil–water interface than without, indicating the protein molecules are associated in the bulk. This may result in differences in the interfacial structure, and hence affect the interaction between the train segments. To clarify this, additional experiments are required that observe the interfacial configuration, perhaps in combination with molecular dynamics simulations.

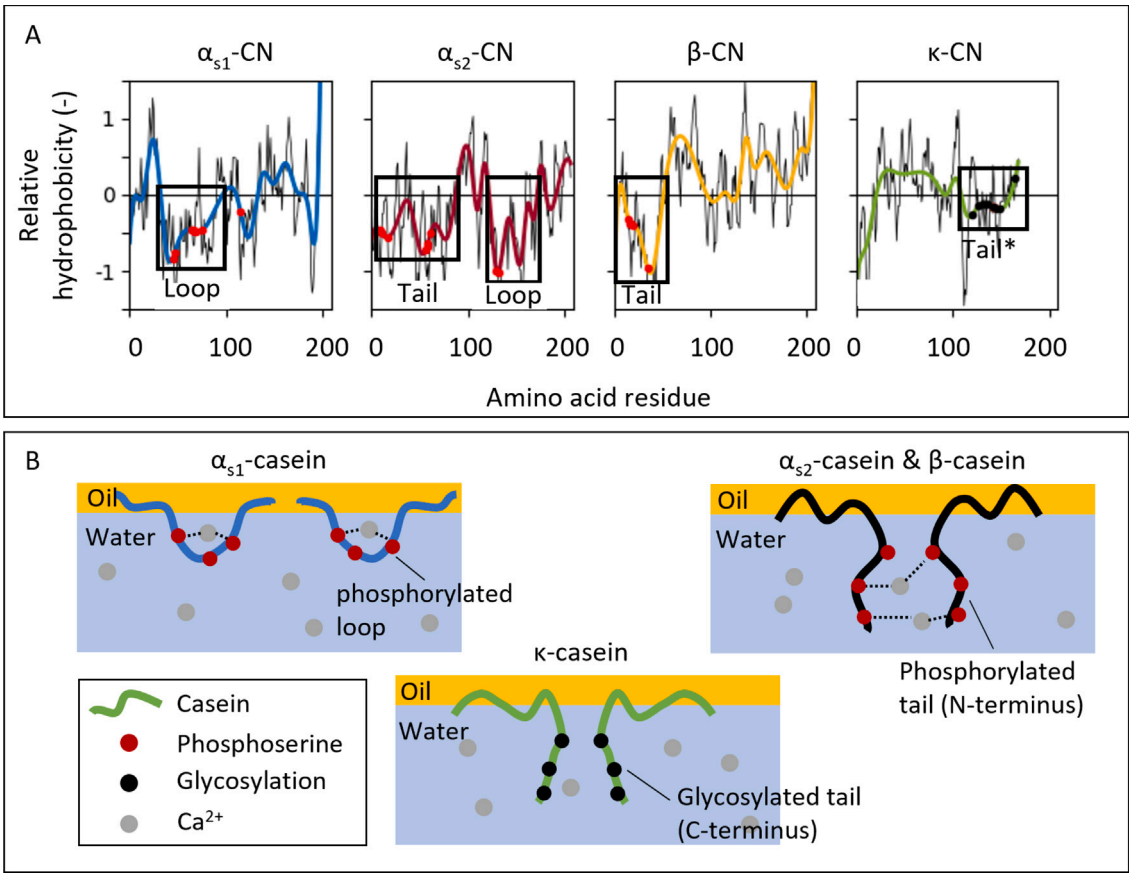

Fig. 3. Distribution of relative hydrophobicity along the amino acid chain of common variants (Bijl et al., 2019) of α_{s1}-CN (var. B-9P, blue), α_{s2}-CN (var. A-10P, red), β-CN (var. A^2-5P, yellow), & κ-CN (var. A-1P, green) (A). The colored lines are a guide to the eye and the black lines are the actual hydrophobicity, hydrophilic regions are highlighted. The hydrophobicity was calculated according to the Cowan–Whittaker hydrophobicity by averaging over the neighboring amino acid residues (Cowan & Whittaker, 1990). Since phosphorylation and glycosylation are not taken into account for this hydrophobicity scale, these groups are indicated with red and black points, respectively. A schematic of Ca^{2+} interactions with the different casein fractions (B). The α_{s1}-CN is hypothesized to form a loop that mainly forms intramolecular Ca^{2+} bridges, α_{s2}- and β-CN form intermolecular Ca^{2+} bridges between tails, and κ-CN does not form Ca^{2+} bridges. *C-terminal end of κ-CN is hydrophilic due to heavy glycosylation (Bijl et al., 2019; de Kruif & Zhulina, 1996; Walstra & Jennes, 1984), which could not be taken into account with this method.

3.3. Binary blends of Casein

With the individual casein fractions characterized, we continued mapping the interactions between different caseins. Therefore, we made binary blends of all casein fractions and compared the dilatational storage modulus of the binary blend and the individual fractions. The fractions were blended in the ratio as they occur in milk (4:1.1:3.8:1.3) (Davies & Law, 1977), for example the ratio of α_{s1}: α_{s2} was 4:1.1 while the total protein concentration was fixed. In Table 3, the modulus of the single component interface is shown on the diagonal and the blends are shown off-diagonal. In each row the modulus of the single component interface is compared with the blends and a cell is colored green if the modulus increases and red when it decreases. Remarkable is that the addition of β-CN results in a reduction of the modulus of all casein fractions. For α_{s2}- and κ-CN, the resulting modulus is even lower than that of β-CN. This shows that the interaction between β-CN and α_{s2}-CN or κ-CN is anti-synergistic, in other words the modulus is lower than what can be expected from the average of the individual moduli. Interestingly this is contrary to what was seen for casein at the air–water interface where β-CN dominates over α_{s1}- or α_{s2}-CN and only κ-CN disturbs the β-CN network (de Groot et al., 2024). These results point to a fundamental difference in interface stabilization between air–water and oil–water interfaces, possibly related to the difference in dielectric constant, protrusion depth, or hydrophobicity, as explained before. The anti-synergy is unique to β-CN, the other fractions have a synergistic effect in a binary blend. Those combinations show an increase in modulus compared to the single component interface. It should be noted that most changes are not significant, so we should be careful to draw conclusions on just one ratio. However, it seems evident that the aforementioned trends capture the general behavior of binary casein blends.

Often, the disruptive effect of blending is highly dependent on concentration. The adsorption rate is closely related to concentration but plateaus at higher concentrations as shown by Xu and Damodaran (1994) for β-CN. At low concentrations, components can arrive sequentially at the interface whereas at high concentrations they arrive shortly after each other or even simultaneously. Therefore, we also test the effect of β-CN at a protein concentration of 0.1%. The increase in total protein concentration from 0.01% to 0.1% showed an increasing disturbance by β-CN while the modulus of the single component interfaces remained unchanged at a higher concentration (SI, Fig. S2). In Table 4, it is shown that a blend of β-CN with α_{s1}-CN, α_{s2}-CN, or κ-CN has a lower modulus than only β-CN. This confirms the anti-synergetic effect of β-CN observed at 0.01%. It is challenging to hypothesize about what exact mechanism is responsible for the incompatibility of a β-CN blend. However, literature reports in-plane phase separation for a binary blend of β- and α_{s1}-CN (Damodaran & Sengupta, 2003; Sengupta et al., 2000) which could be a reason for the anti-synergistic effect we observe.

3.4. Complete Casein blend

From the binary blends we now focus on a complete blend of casein where the casein fractions are blended in the ratio they naturally occur in bovine milk (4:1.1:3.8:1.3) (Davies & Law, 1977). Here, we assess

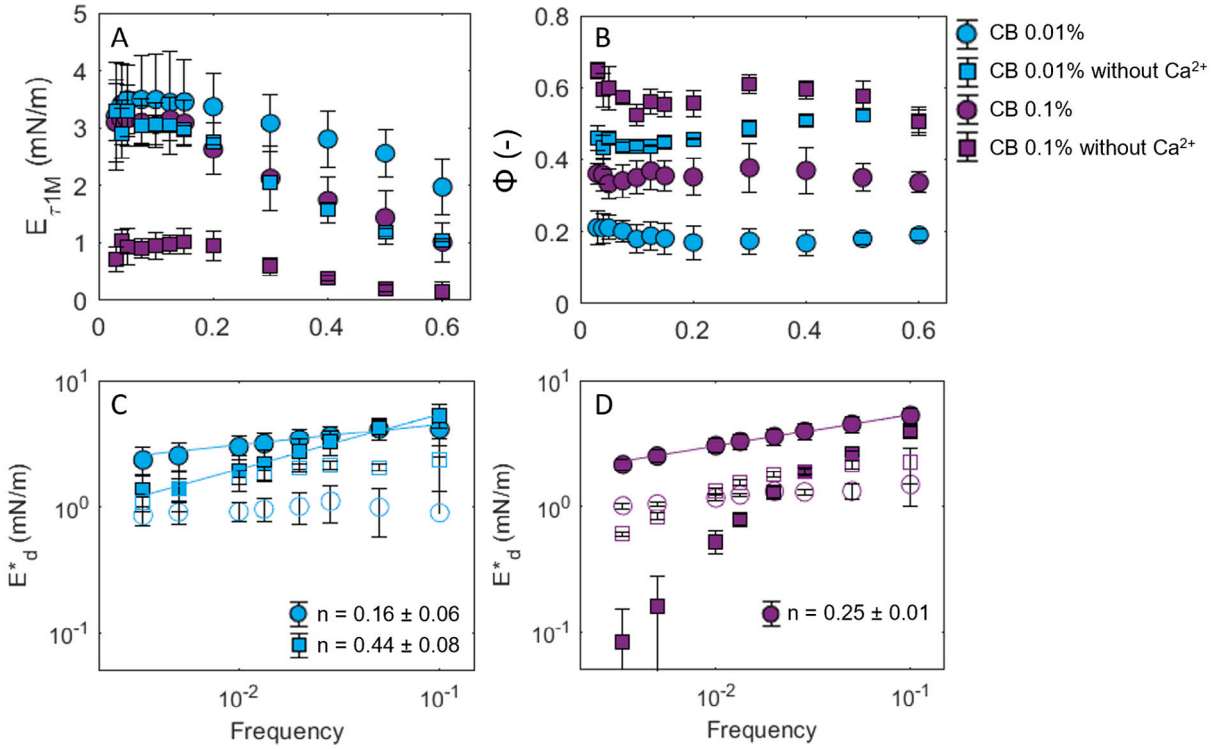

Fig. 4. Strain sweep (plot A & B) and frequency sweep (plot C & D) of a complete casein blend. A casein blend in SMUF with (circle) and without Ca^{2+} (square) is shown at 0.01% (blue) and 0.1% w/w protein (purple). The storage modulus of the frequency sweeps is fitted with a power law ($E'_d \sim \omega^n$), open symbols show the loss modulus.

the interfacial functionality at 0.01% and 0.1% protein in Fig. 4. The interfacial stiffness is characterized with $E_{\tau 1M}$, and the stiffness at low deformation is ~ 3.5 mN/m for 0.01% protein. This is comparable to the stiffness of β-CN (~ 3.3 mN/m) and confirms the anti-synergy of β-CN as this is lower than the weighted average of the individual fractions (4.8 mN/m). This was confirmed by measuring a blend without β-CN, which had a higher modulus (~ 4.6 mN/m, SI Fig. S3 A) than the casein blend. When Ca^{2+} is removed, the stiffness decreases, especially at larger deformations. This indicates that the network formation at 0.01% depends on the presence of Ca^{2+} and that the absence of Ca^{2+} makes the interface less stiff and more brittle. In the Lissajous plots (SI, Fig. S4), we see that at 50% deformation the removal of Ca^{2+} results in a more viscous response with a lower slope. The viscous behavior is quantified with the dissipation ratio in Fig. 4 B. This figure shows that removing Ca^{2+} results in an increased dissipation ratio from 0.2 to 0.5. The response of the interface becomes more plastic because of reduced in-plane interactions, making the casein molecules more mobile. At 0.1%, similar behavior is observed but with more pronounced effects, just like in the binary blends. The anti-synergetic effect of blending casein is stronger at 0.1%, the stiffness is lower than at 0.01% (small deformations: ~ 3 vs ~ 3.3 mN/m). If we then look at the dissipation ratio we also see an increase from 0.2 at 0.01% to 0.4 at 0.1%. The increase in concentration has created more disturbance in the interfacial network which makes it less stiff with a more dominant viscous response. The removal of Ca^{2+} is even more detrimental to the interfacial stiffness ($E_{\tau 1M}$) than at 0.01%, the stiffness decreases to ~ 1 mN/m and the dissipation ratio (Φ) increases from ~ 0.4 to ~ 0.6. This shows that the response of the interface becomes less stiff and more plastic because there is nearly no residual casein network.

In general, a less well-established network will result in more exchange between bulk and interface (de Groot et al., 2023). Therefore, frequency sweeps were performed and are shown in Fig. 4 C & D. The casein blend at 0.01% in SMUF shows power law-behavior (n=0.16 ± 0.06), whereas in the absence of Ca^{2+} the exponent is close to Lucassen-van den Tempel behavior (n=0.44 ± 0.08). The high exponent confirms our observations of the strain sweep, Ca^{2+} is the main driver for the formation of interfacial network through in-plane interactions. It should be noted that the Lucassen-van den Tempel model Eq. (3) could not be fitted to the complex modulus of the casein blend at 0.01% without Ca^{2+}. Hence, this indicates that the complex modulus is in fact not only established by limited bulk-interface exchange as was described by Lucassen and van den Tempel (Lucassen & Van Den Tempel, 1972). For an explanation and a more extreme display of this effect we turn to the casein blend at 0.1%. Here, we observe a higher frequency dependence of the casein blend in SMUF compared to 0.01%. Because of the reduced network formation, as observed in the strain sweep, bulk-interface exchange becomes more important for the interfacial complex modulus. This increases exponent for the frequency dependence to n=0.25 ± 0.01 (Fig. 4 D). Now when Ca^{2+} is removed, the 'glue' of the network is gone and the interfacial structure collapses. The frequency sweep shows an extremely high dependence on frequency with a crossover of the loss and storage modulus at ~ 0.03 Hz. The frequency dependence is higher than what can be described by the Lucassen-van den Tempel model (n=0.5), this behavior seems closer to Maxwell behavior as is seen in bulk rheology. Maxwell behavior describes a quadratic dependence of the storage modulus before the crossover point of loss and storage modulus Eq. (4). The fitting of a Maxwell-model or a multi mode Maxwell-model however did not describe our data accurately. Despite this, a casein blend without Ca^{2+} seems to behave more like a viscous polymer blend than an interfacial protein network. This emphasizes the importance of Ca^{2+} for the formation of an interfacial network and shows that the anti-synergetic effect becomes more important at high casein concentrations.

The effect of casein blending depends on the casein fractions involved, but many blends result in a decreased interfacial network formation which is accelerated in the absence of Ca^{2+}. Hence, for future work on recombinant casein variants it might be more interesting to look at individual functionality instead of a blend as interfacial stiffness probably will diminish in a blend of casein fractions.

4. Conclusions

The individual casein (CN) fractions α_{s1}-CN, α_{s2}-CN, β-CN, & κ-CN show disordered solid-like viscoelastic behavior in the presence of Ca^{2+} at oil–water interfaces. In the absence of Ca^{2+}, α_{s2}- and β-CN form a weaker interface, whereas α_{s1}-CN forms a stiffer interface, and κ-CN is unaffected. The difference in calcium sensitivity was related to the interfacial configuration. α_{s1}-CN is the only fraction with a train-loop-train configuration which makes it less capable of forming inter-molecular calcium bridges. Contrarily α_{s2}-CN and β-CN have a tail protruding into the hydrophilic sub phase that contains many phosphoserine residues and appear to be capable of forming interfacial networks through calcium bridges between tails. Finally, the κ-CN has no phosphoserine residue in the tail, thereby being insensitive to Ca^{2+}.

Binary blends of casein fractions revealed anti-synergy induced by β-CN that inhibits interfacial network formation. The addition of β-CN reduced the storage modulus of the binary blend to below the modulus of each individual fraction. Within a complete casein blend this effect persisted, as a blend of α_{s1}-CN, α_{s2}-CN, β-CN, & κ-CN (ratio 4:1.1:3.8:1.3) had a low interfacial stiffness. The stiffness of the complete casein blend was comparable to the stiffness of β-CN at 0.01%. At higher concentrations, the network was disturbed as the stiffness decreased and the dissipation ratio increased. In the absence of Ca^{2+}, the interfacial network was nearly completely broken down resulting in highly viscous behavior. The interfacial viscoelasticity was comparable to polymer behavior instead of an interfacial protein network.

With this work we show how individual casein fractions interact at the oil–water interface. The presence of β-CN has a detrimental effect on the modulus of a casein blend especially at higher concentrations. Moreover, the formation of an interfacial network requires Ca^{2+}, and in its absence the interfacial modulus is much lower, because of an absence of inter-molecular calcium bridges. This provides a template for the development of recombinant caseins for emulsions, and in particular shows that blending of casein fractions is not advised, as that decreases interfacial network formation. The preferred fraction for stabilization depends on the requirements: when fast emulsification is required, β-CN is most promising, while for stability α_{s1} is a most promising candidate, since it forms a stiff disordered solid-like interface.

CRediT authorship contribution statement

A. de Groot: Writing – original draft, Methodology, Investigation, Formal analysis, Conceptualization. **E. Bijl:** Writing – review & editing, Supervision, Methodology, Funding acquisition, Conceptualization. **L.M.C. Sagis:** Writing – review & editing, Supervision, Methodology, Funding acquisition, Conceptualization.

Declaration of competing interest

The authors declare that they have no known competing financial interests or personal relationships that could have appeared to influence the work reported in this paper.

Acknowledgments

This publication is part of the 'Animal-free milk proteins' project (with project number NWA.1292.19.302) of the NWA research programme 'Research along Routes by Consortia (ORC)', which is funded by the Dutch Research Council (NWO).

Appendix A. Supplementary data

Supplementary material related to this article can be found online at https://doi.org/10.1016/j.foodhyd.2024.110741.

Data availability

Data will be made available on request.

References

Aoki, T., Toyooka, K., & Kako, Y. (1985). Role of phosphate groups in the calcium sensitivity of αs2-casein. *Journal of Dairy Science*, *68*(7), 1624–1629. http://dx.doi.org/10.3168/jds.S0022-0302(85)81005-5.

Aoki, T., Umeda, T., & Kako, Y. (1992). The least number of phosphate groups for crosslinking of casein by colloidal calcium phosphate. *Journal of Dairy Science*, *75*(4), 971–975. http://dx.doi.org/10.3168/jds.S0022-0302(92)77838-2.

Bergfreund, J., Bertsch, P., & Fischer, P. (2021). Adsorption of proteins to fluid interfaces: Role of the hydrophobic subphase. *Journal of Colloid and Interface Science*, *584*, 411–417. http://dx.doi.org/10.1016/j.jcis.2020.09.118.

Bergfreund, J., Bertsch, P., & Fischer, P. (2021). Effect of the hydrophobic phase on interfacial phenomena of surfactants, proteins, and particles at fluid interfaces. *Current Opinion in Colloid & Interface Science*, *56*, Article 101509. http://dx.doi.org/10.1016/j.cocis.2021.101509.

Bijl, E., Holland, J. W., & Boland, M. (2019). Posttranslational modifications of caseins. *Milk proteins: from expression to food* (3). (pp. 173–211). Elsevier Inc., http://dx.doi.org/10.1016/B978-0-12-815251-5.00005-0.

Bonfatti, V., Grigoletto, L., Cecchinato, A., Gallo, L., & Carnier, P. (2008). Validation of a new reversed-phase high-performance liquid chromatography method for separation and quantification of bovine milk protein genetic variants. *Journal of Chromatography A*, *1195*(1–2), 101–106. http://dx.doi.org/10.1016/j.chroma.2008.04.075.

Cano-Ruiz, M., & Richter, R. (1997). Effect of homogenization pressure on the milk fat globule membrane proteins. *Journal of Dairy Science*, *80*(11), 2732–2739. http://dx.doi.org/10.3168/jds.S0022-0302(97)76235-0.

Chrysanthou, A., Bosch-Fortea, M., Zarbakhsh, A., & Gautrot, J. E. (2023). Interfacial mechanics of b-casein and albumin mixed protein assemblies at liquid-liquid interfaces. http://dx.doi.org/10.26434/chemrxiv-2023-m29g4, preprint ChemRxiv.

Cowan, R., & Whittaker, R. G. (1990). Hydrophobicity indices for amino acid residues as determined by high-performance liquid chromatography. *Peptide Research*, *3*(2), 75–80.

Dalgleish, D. G. (1993). The sizes and conformations of the proteins in adsorbed layers of individual caseins on latices and in oil-in-water emulsions. *Colloids and Surfaces B (Biointerfaces)*, *1*(1), 1–8. http://dx.doi.org/10.1016/0927-7765(93)80011-M.

Damodaran, S., & Sengupta, T. (2003). Dynamics of competitive adsorption of αs-casein and β-casein at planar triolein-water interface: Evidence for incompatibility of mixing in the interfacial film. *Journal of Agricultural and Food Chemistry*, *51*(6), 1658–1665. http://dx.doi.org/10.1021/jf020784v.

Darling, D. F., & Butcher, D. W. (1978). Milk-fat globule membrane in homogenized cream. *Journal of Dairy Research*, *45*(2), 197–208. http://dx.doi.org/10.1017/S002202990001637X.

Davies, D. T., & Law, A. J. (1977). The composition of whole casein from the milk of Ayrshire cows. *Journal of Dairy Research*, *44*(3), 447–454. http://dx.doi.org/10.1017/S0022029900020410.

de Groot, A., Bijl, E., & Sagis, L. (2024). Interfacial network formation by casein blends in the presence of Ca2+ is dominated by β- and κ-casein. *Food Hydrocolloids*, *154*, Article 110085. http://dx.doi.org/10.1016/j.foodhyd.2024.110085.

de Groot, A., Yang, J., & Sagis, L. M. (2023). Surface stress decomposition in large amplitude oscillatory interfacial dilatation of complex interfaces. *Journal of Colloid and Interface Science*, *638*, 569–581. http://dx.doi.org/10.1016/j.jcis.2023.02.007.

de Kruif, C., & Zhulina, E. B. (1996). κ-casein as a polyelectrolyte brush on the surface of casein micelles. *Colloids and Surfaces A: Physicochemical and Engineering Aspects*, *117*(1–2), 151–159. http://dx.doi.org/10.1016/0927-7757(96)03696-5.

de Vries, R., van Knegsel, A., Johansson, M., Lindmark-Månsson, H., van Hooijdonk, T., Holtenius, K., & Hettinga, K. (2015). Effect of shortening or omitting the dry period of Holstein-Friesian cows on casein composition of milk. *Journal of Dairy Science*, *98*(12), 8678–8687. http://dx.doi.org/10.3168/jds.2015-9544.

Diaz-Bustamante, M. L., Keppler, J. K., Reyes, L. H., & Alvarez Solano, O. A. (2023). Trends and prospects in dairy protein replacement in yogurt and cheese. *Heliyon*, *9*(6), Article e16974. http://dx.doi.org/10.1016/j.heliyon.2023.e16974.

Dickinson, E., Horne, D. S., Pinfield, V. J., & Leermakers, F. A. (1997). Self-consistent-field modelling of casein adsorption. Comparison of results for αs1-casein and β-casein. *Journal of the Chemical Society - Faraday Transactions*, *93*(3), 425–432. http://dx.doi.org/10.1039/a604864a.

Dickinson, E., Rolfe, S. E., & Dalgleish, D. G. (1988). Competitive adsorption of αs1-casein and β-casein in oil-in-water emulsions. *Topics in Catalysis*, *2*(5), 397–405. http://dx.doi.org/10.1016/S0268-005X(88)80004-3.

Dumpler, J. (2018). *Heat stability of concentrated milk systems*. Wiesbaden: Springer Fachmedien Wiesbaden, http://dx.doi.org/10.1007/978-3-658-19696-7.

Ewoldt, R. H., Winter, P., Maxey, J., & McKinley, G. H. (2010). Large amplitude oscillatory shear of pseudoplastic and elastoviscoplastic materials. *Rheologica Acta*, *49*(2), 191–212. http://dx.doi.org/10.1007/s00397-009-0403-7.

Fainerman, V. B., Aksenenko, E. V., Makievski, A. V., Trukhin, D. V., Yeganehzad, S., Gochev, G., & Miller, R. (2020). Surface tension and dilational rheology of mixed β-casein – β-lactoglobulin aqueous solutions at the water/air interface. *Food Hydrocolloids*, *106*(March), Article 105883. http://dx.doi.org/10.1016/j.foodhyd.2020.105883.

Food and Agriculture Organization (2010). *Greenhouse gas emissions from the dairy sector: Technical Report 1 International organization 1 (1)*, Food and Agriculture Organization.

Fox, P. F., Uniacke-Lowe, T., McSweeney, P. L. H., & O'Mahony, J. A. (2015). *Dairy chemistry and biochemistry*. Cham: Springer International Publishing, http://dx.doi.org/10.1007/978-3-319-14892-2.

Graham, D. E., & Phillips, M. C. (1979). Proteins at liquid interfaces. I. Kinetics of adsorption and surface denaturation. *Journal of Colloid and Interface Science*, *70*(3), 403–414. http://dx.doi.org/10.1016/0021-9797(79)90048-1.

Hansson, L., Bergstrom, S., Hernell, O., Lonnerdal, B., Nilsson, A., & Stromqvist, M. (1993). Expression of human milk β-casein in Escherichia coli: Comparison of recombinant protein with native isoforms. *Protein Expression and Purification*, *4*(5), 373–381. http://dx.doi.org/10.1006/prep.1993.1049.

Harton, K., & Shimizu, S. (2019). Statistical thermodynamics of casein aggregation: Effects of salts and water. *Biophysical Chemistry*, *247*, 34–42. http://dx.doi.org/10.1016/j.bpc.2019.02.004.

Hettinga, K., & Bijl, E. (2022). Can recombinant milk proteins replace those produced by animals? *Current Opinion in Biotechnology*, *75*, Article 102690. http://dx.doi.org/10.1016/j.copbio.2022.102690.

Holland, J. W., Deeth, H. C., & Alewood, P. F. (2006). Resolution and characterisation of multiple isoforms of bovine κ-casein by 2-DE following a reversible cysteine-tagging enrichment strategy. *PROTEOMICS*, *6*(10), 3087–3095. http://dx.doi.org/10.1002/pmic.200500780.

Horne, D. S. (2020). Casein micelle structure and stability. In *Milk proteins* (pp. 213–250). Elsevier, http://dx.doi.org/10.1016/B978-0-12-815251-5.00006-2.

Horne, D., & Dalgleish, D. (1980). Electrostatic interaction and the kinetics of protein aggregation: αs1-casein. *International Journal of Biological Macromolecules*, *2*(3), 154–160. http://dx.doi.org/10.1016/0141-8130(80)90067-7.

Huppertz, T. (2013). Chemistry of the caseins, In P. L. H. McSweeney, & P. F. Fox (Eds.), *Advanced dairy chemistry: vol. 1A*, (4). (pp. 135–160). Boston, MA: Springer US, http://dx.doi.org/10.1007/978-1-4614-4714-6.

Husband, F. A., Wilde, P. J., Mackie, A. R., & Garrood, M. J. (1997). A comparison of the functional and interfacial properties of β-casein and dephosphorylated β-casein. *Journal of Colloid and Interface Science*, *195*(1), 77–85. http://dx.doi.org/10.1006/jcis.1997.5137.

Iametti, S., Versuraro, L., Tragna, S., Giangiacomo, R., & Bonomi, F. (1997). Surface properties of the fat globule in treated creams. *International Dairy Journal*, *7*(6–7), 375–380. http://dx.doi.org/10.1016/S0958-6946(97)00039-3.

Jennes, R., & Koops, J. (1962). Preparation and properties of a salt solution which simulates milk ultrafiltrate. (1). *Netherlands Milk and Dairy Journal*, *16*, 153–164.

Jin, Y., Liu, D., & Hu, J. (2021). Effect of surfactant molecular structure on emulsion stability investigated by interfacial dilatational rheology. *Polymers*, *13*(7), 1127. http://dx.doi.org/10.3390/polym13071127.

Langevin, D. (2000). Influence of interfacial rheology on foam and emulsion properties. *Advances in Colloid and Interface Science*, *88*(1–2), 209–222. http://dx.doi.org/10.1016/S0001-8686(00)00045-2.

Li, M., Auty, M. A., Crowley, S. V., Kelly, A. L., O'Mahony, J. A., & Brodkorb, A. (2019). Self-association of bovine β-casein as influenced by calcium chloride, buffer type and temperature. *Food Hydrocolloids*, *88*, 190–198. http://dx.doi.org/10.1016/j.foodhyd.2018.09.035.

Li, M., O'Mahony, J. A., Kelly, A. L., & Brodkorb, A. (2020). The influence of temperature- and divalent-cation-mediated aggregation of β-casein on the physical and microstructural properties of β-casein-stabilised emulsions. *Colloids and Surfaces B (Biointerfaces)*, *187*, http://dx.doi.org/10.1016/j.colsurfb.2019.110620.

Loch, J. I., Bonarek, P., Tworzydło, M., Polit, A., Hawro, B., Ł ach, A., Ludwin, E., & Lewiński, K. (2016). Engineered β-Lactoglobulin produced in E. coli: Purification, biophysical and structural characterisation. *Molecular Biotechnology*, *58*(10), 605–618. http://dx.doi.org/10.1007/s12033-016-9960-z.

Lucassen, J., & Van Den Tempel, M. (1972). Dynamic measurements of dilational properties of a liquid interface. *Chemical Engineering Science*, *27*(6), 1283–1291. http://dx.doi.org/10.1016/0009-2509(72)80104-0.

Mccrae, C. H. (1994). Homogenization of milk emulsions:use of microfluidizer. *International Journal of Dairy Technology*, *47*(1), 28–31. http://dx.doi.org/10.1111/j.1471-0307.1994.tb01267.x.

Miller, R., Ferri, J. K., Javadi, A., Krägel, J., Mucic, N., & Wüstneck, R. (2010). Rheology of interfacial layers. *Colloid and Polymer Science*, *288*(9), 937–950. http://dx.doi.org/10.1007/s00396-010-2227-5.

Poore, J., & Nemecek, T. (2018). Reducing foods environmental impacts through producers and consumers. *Science*, *360*(6392), 987–992. http://dx.doi.org/10.1126/science.aaq0216.

Sagis, L. M. C. (2011). Dynamic properties of interfaces in soft matter: Experiments and theory. *Reviews of Modern Physics*, *83*(4), 1367–1403. http://dx.doi.org/10.1103/RevModPhys.83.1367.

Sengupta, T., Razumovsky, L., & Damodaran, S. (2000). Phase separation in two-dimensional αs-casein/β-casein/water ternary film at the air-water interface. *Langmuir*, *16*(16), 6583–6589. http://dx.doi.org/10.1021/la991452w.

Swaisgood, H. E. (1993). Review and update of casein chemistry. *Journal of Dairy Science*, *76*(10), 3054–3061. http://dx.doi.org/10.3168/jds.S0022-0302(93)77645-6.

Thorn, D. C., Ecroyd, H., Carver, J. A., & Holt, C. (2015). Casein structures in the context of unfolded proteins. *International Dairy Journal*, *46*, 2–11. http://dx.doi.org/10.1016/j.idairyj.2014.07.008.

Velev, O. D., Campbell, B. E., & Borwankar, R. P. (1998). Effect of calcium ions and environmental conditions on the properties of β-casein stabilized films and emulsions. *Langmuir*, *14*(15), 4122–4130. http://dx.doi.org/10.1021/la980212y.

Walstra, P., & Jennes, R. (1984). *Dairy chemistry and physics*. Wiley.

White, J. R. (2006). Polymer ageing: physics, chemistry or engineering? Time to reflect. *Comptes Rendus de l'Academie des Sciences, Serie II*, *9*(11–12), 1396–1408. http://dx.doi.org/10.1016/j.crci.2006.07.008.

Wüstneck, R., Fainerman, V. B., Aksenenko, E. V., Kotsmar, C., Pradines, V., Krägel, J., & Miller, R. (2012). Surface dilatational behavior of β-casein at the solution/air interface at different pH values. *Colloids and Surfaces A: Physicochemical and Engineering Aspects*, *404*, 17–24. http://dx.doi.org/10.1016/j.colsurfa.2012.03.050.

Xu, S., & Damodaran, S. (1994). Kinetics of adsorption of proteins at the air-water interface from a binary mixture. *Langmuir*, *10*(2), 472–480. http://dx.doi.org/10.1021/la00014a022.

Zhou, X., Yang, J., Sala, G., & Sagis, L. M. (2022). Are micelles actually at the interface in micellar casein stabilized foam and emulsions? *Food Hydrocolloids*, *129*(February), Article 107610. http://dx.doi.org/10.1016/j.foodhyd.2022.107610.